

Percolation in interdependent and interconnected networks: Abrupt change from second- to first-order transitions

Yanqing Hu,^{1,2,3} Baruch Ksherim,² Reuven Cohen,^{2,4} and Shlomo Havlin²

¹*School of Mathematics, Southwest Jiaotong University, Chengdu 610031, China*

²*Department of Physics, Bar-Ilan University, Ramat-Gan 52900, Israel*

³*Department of Systems Science, School of Management and Center for Complexity Research, Beijing Normal University, Beijing 100875, China*

⁴*Department of Mathematics, Bar-Ilan University, Ramat-Gan 52900, Israel*

(Received 14 June 2011; revised manuscript received 13 October 2011; published 20 December 2011)

Robustness of two coupled networks systems has been studied separately only for dependency coupling [Buldyrev *et al.*, *Nature (London)* **464**, 1025 (2010)] and only for connectivity coupling [Leicht and D'Souza, e-print [arXiv:0907.0894](https://arxiv.org/abs/0907.0894)]. Here we study, using a percolation approach, a more realistic coupled networks system where both interdependent and interconnected links exist. We find rich and unusual phase-transition phenomena including *hybrid* transition of mixed first and second order, i.e., discontinuities like in a first-order transition of the giant component followed by a continuous decrease to zero like in a second-order transition. Moreover, we find unusual discontinuous changes from second-order to first-order transition as a function of the dependency coupling between the two networks.

DOI: [10.1103/PhysRevE.84.066116](https://doi.org/10.1103/PhysRevE.84.066116)

PACS number(s): 89.75.Hc, 64.60.ah, 89.75.Fb

I. INTRODUCTION

During the last decade complex networks have been studied intensively, where most of the research was devoted to analyzing the structure and functionality of isolated systems modeled as single noninteracting networks [1–25]. However, most real networks are not isolated, as they either complement other networks (“interconnected networks”), must consume resources supplied by other networks (“interdependent networks”), or both [26–30]. Thus, real networks continuously interact with each other, composing a large complex system, and, with the enhanced development of technology, the coupling between many networks becomes more complex and more significant.

Until now two different types of coupled networks models have been studied. Buldyrev *et al.* [31] investigated the robustness of coupled systems with only interdependence links. In these systems, when a node of one network fails, its dependent counterpart node in the other network also fails. They found that this interdependence makes the system significantly more *vulnerable* [31,32]. At the same time, Leicht and D'Souza [33] studied the case where only connectivity links couple the networks, i.e., interconnected networks, and found that the interconnected links make the system significantly more *robust*. However, real coupled networks often contain both types of links, interdependent as well as interconnected links. For example, the airport and the railway networks in Europe are two coupled networks composing a transportation system. In order to arrive to an airport, one usually uses the railway, while people arriving to the country by airport usually use the railway. In this system, if the airport is disabled by some strike or accident, the passengers can still use the nearby railway station and travel to their destination or to another airport by train, so the two networks complement each other and are coupled by connectivity links. On the other hand, if the railway network is disabled, the airport traffic is damaged, and if the airport is disabled, the railway traffic is damaged, so both networks are coupled by dependency links as well. The

important characteristic of such systems is that a failure of nodes in one network carries implications not only for this network but also on the function of other dependent networks. In this way it is possible to have cascading failures between the coupled networks that may lead to a catastrophic collapse of the whole system. Nevertheless, small clusters disconnected from the giant component in one network can still function through interconnected links connecting them to the giant component of the other network. Thus, we have two competing effects; the interconnectivity links *increase* the robustness of the system, while the interdependency links *decrease* its robustness. Here we study the competition of the two types of interlinks on the system robustness using a percolation approach, and we find unusual types of percolation phase transitions.

II. GENERAL FRAMEWORK

Let us consider a system of two networks, A and B , which are coupled by both dependency and connectivity links (see Fig. 1). The two networks are partially coupled by dependency links, so that a fraction q_A of A nodes depends on nodes in network B , and a fraction q_B of B nodes depends on the nodes in network A , with the following two assumptions: that a node from one network depends on no more than one node from the other network and that, if node A_i depends on node B_j , then if B_j depends on some A_h then $h = i$ (Fig. 1). In addition, the connectivity links within each network and between the networks can be described by a set of degree distributions $\{\rho_{k_A, k_{AB}}^A, \rho_{k_B, k_{BA}}^B\}$, where $\rho_{k_A, k_{AB}}^A$ ($\rho_{k_B, k_{BA}}^B$) denotes the probability of an A node (B node) to have k_A (k_B) links to other A nodes (B node) and k_{AB} (k_{BA}) links toward B nodes (A nodes). In this manner we get a two-dimensional generating function describing all the connectivity links [33], $\mathcal{G}_0^A(x_A, x_B) = \sum_{k_A, k_{AB}} \rho_{k_A, k_{AB}}^A x_A^{k_A} x_B^{k_{AB}}$, and $\mathcal{G}_0^B(x_A, x_B) = \sum_{k_B, k_{BA}} \rho_{k_B, k_{BA}}^B x_A^{k_{BA}} x_B^{k_B}$.

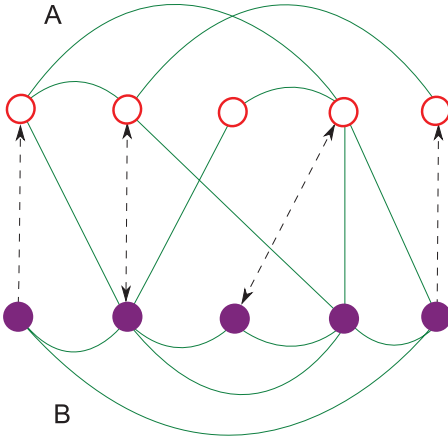


FIG. 1. (Color online) Two types of interlinks where the dependency links (dashed arrows) are not necessarily bidirectional. The nodes of A and B are randomly connected with *connectivity links* (full line). The functionality of some of the A nodes (red open circles) depends on B nodes (purple solid circles) and vice versa.

The cascading process is initiated by randomly removing a fraction $1 - p$ of the A nodes and all their connectivity links. Because of the interdependence between the networks, the nodes in network B that depend on the removed A nodes are also removed along with their connectivity links. As nodes and links are removed, each network breaks up into connected components (clusters). We assume that when the network is fragmented the nodes belonging to the largest component (called the giant component) represent a finite fraction of the network which is still functional, while nodes that are parts of the remaining smaller clusters become dysfunctional, *unless* there exists a path of connectivity links connecting these small clusters to the largest component of the other network. Since the networks have different topologies, the removal of nodes and related dependency links is not symmetric in both networks, so that a cascading process occurs, until the system either becomes fragmented or stabilizes with a giant component.

Let $g_A(\varphi, \phi)$ and $g_B(\varphi, \phi)$ be the fractions of A nodes and B nodes in the giant components after the percolation process initiated by removing a fraction of $1 - \varphi$ and $1 - \phi$ of networks A and B, respectively [11]. The functions $g_A(\varphi, \phi)$ and $g_B(\varphi, \phi)$ depend only on $\mathcal{G}_0^A(x_A, x_B)$ and $\mathcal{G}_0^B(x_A, x_B)$ (for details see the Appendix), and the dynamics of the cascading process can be described by the following set of equations:

$$\begin{aligned} \varphi_1 &= p, & \phi_1 &= 1, & P_1^A &= \varphi_1 g_A(\varphi_1, \phi_1), \\ \phi_2 &= 1 - q_B [1 - p g_A(\varphi_1, \phi_1)], & P_2^B &= \phi_2 g_B(\varphi_1, \phi_2), \\ \varphi_2 &= p \{1 - q_A [1 - g_B(\varphi_1, \phi_2)]\}, & P_2^A &= \varphi_2 g_A(\varphi_2, \phi_2), \\ \phi_3 &= 1 - q_B [1 - p g_A(\varphi_2, \phi_2)], & P_3^B &= \phi_3 g_B(\varphi_2, \phi_3), \end{aligned} \quad (1)$$

where φ_i, ϕ_i are the remaining fractions of nodes at stage i of the cascade of failures and P_i^A, P_i^B are the corresponding giant components of networks A and B at the cascading stage i , respectively. Generally, the n th step is given by the

equations

$$\begin{aligned} \varphi_n &= p \{1 - q_A [1 - g_B(\varphi_{n-1}, \phi_n)]\}, \\ \phi_n &= 1 - q_B [1 - p g_A(\varphi_{n-1}, \phi_{n-1})], \\ P_n^A &= \varphi_n g_A(\varphi_n, \phi_n), & P_n^B &= \phi_n g_B(\varphi_{n-1}, \phi_n). \end{aligned} \quad (2)$$

By introducing two new notations,

$$u_A \equiv g_A(\varphi_\infty, \phi_\infty), \quad u_B \equiv g_B(\varphi_\infty, \phi_\infty), \quad (3)$$

we can write Eqs. (2) at the end of the cascading process, $n \rightarrow \infty$, as

$$\varphi_\infty = p [1 - q_A (1 - u_B)], \quad \varphi_\infty = 1 - q_B (1 - p u_A), \quad (4)$$

and the giant components are

$$\begin{aligned} P_\infty^A &= u_A \varphi_\infty = u_A p [1 - q_A (1 - u_B)], \\ P_\infty^B &= u_B \varphi_\infty = u_B [1 - q_B (1 - p u_A)]. \end{aligned} \quad (5)$$

III. POISSONIAN DEGREE DISTRIBUTIONS

We consider the case where all degree distributions of the connectivity intra- and interlinks are *Poissonian*, for which the functions u_A and u_B obtain a simple form. Assuming \bar{k}_A and \bar{k}_B are the average intralink degrees in networks A and B and $\bar{k}_{AB}, \bar{k}_{BA}$ are the average interconnectivity links degrees between A and B (allowing the case $\bar{k}_{AB} \neq \bar{k}_{BA}$, since the two networks may be of different sizes), we obtain

$$\begin{aligned} u_A &= 1 - e^{-\bar{k}_A p u_A [1 - q_A (1 - u_B)] - \bar{k}_{AB} u_B [1 - q_B (1 - p u_A)]}, \\ u_B &= 1 - e^{-\bar{k}_{BA} p u_A [1 - q_A (1 - u_B)] - \bar{k}_{BB} u_B [1 - q_B (1 - p u_A)]}. \end{aligned} \quad (6)$$

Generally, for fixed parameters $\bar{k}_A, \bar{k}_B, \bar{k}_{AB}, \bar{k}_{BA}, q_A, q_B$, and p , it is often impossible to achieve an explicit formula for the giant components P_∞^A and P_∞^B . However, one can still solve Eqs. (6) graphically (numerically) and substitute the numerical solution into Eqs. (5). For simplicity and without loss of generality, we study the case where $\bar{k}_A = \bar{k}_B \equiv \bar{k}$ and $\bar{k}_{AB} = \bar{k}_{BA} \equiv \bar{K}$. Figure 2(a) compares the numerical solutions with the simulation results for P_∞^A and P_∞^B as a function of p , showing that the analytical results of Eqs. (5) and (6) are in excellent agreement with the simulations.

A. Partial dependence

Next we are interested in the properties of the phase transition under random attack, so first we determine the conditions when transition does not occur. This is the case where for a given $q_B < 1$, even if all nodes of network A are removed (i.e., $p = 0$), there still exists a giant component in network B [see circles in Fig. 2(a)] and no phase transition occurs. For Poissonian degree distributions, it is easy to see that, if after the removal of all B nodes that depend on the attacked A nodes the new average intralink degree in network B is less than one, i.e.,

$$\bar{k}_B (1 - q_B) < 1, \quad (7)$$

a phase transition does occur. Therefore, our further analysis is based on condition (7). In addition, from now on, we will set both dependency couplings, q_A and q_B , to be larger than zero.

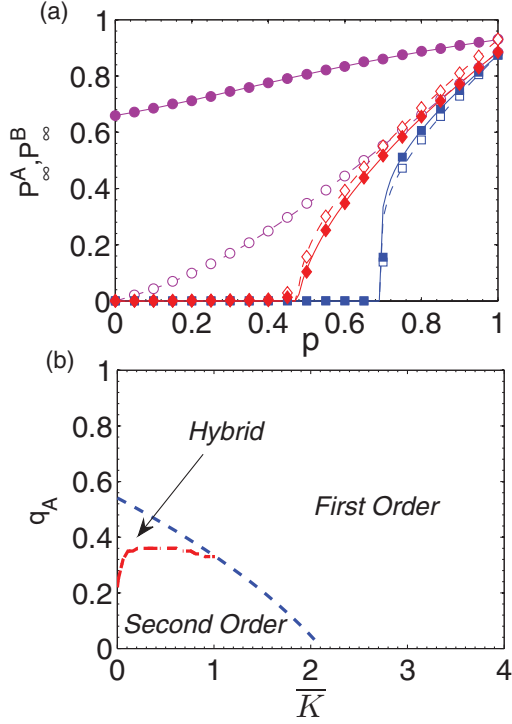


FIG. 2. (Color online) (a) Giant components P_∞^A and P_∞^B vs a fraction of the remaining nodes, p , for $N = 10000$, $\bar{k} = 2$, and $\bar{K} = 1$. Networks A (open symbols) and B (full symbols) are shown for different (q_A, q_B) pairs: $(0.8, 0.1)$ (\circ), $(0.1, 0.8)$ (\diamond), and $(0.8, 0.8)$ (\square). The symbols represent simulations and the lines represent the theory. We see three different types of behaviors: no phase transition (\circ), second-order phase transition (\diamond), and first-order phase transition (\square). (b) Phase diagram showing the first-order, second-order and hybrid phase transition regimes and the boundaries, for $q_B = 1$ and $\bar{k} = 3$. In the second-order transition regime, between the two dashed curves (red and blue), there exists a hybrid phase-transition regime [see details in Fig. 3(c)]. Since the hybrid transition is continuous in the neighborhood of p_c and the jump occurs well above p_c , we classify this hybrid phase transition as a second-order phase transition.

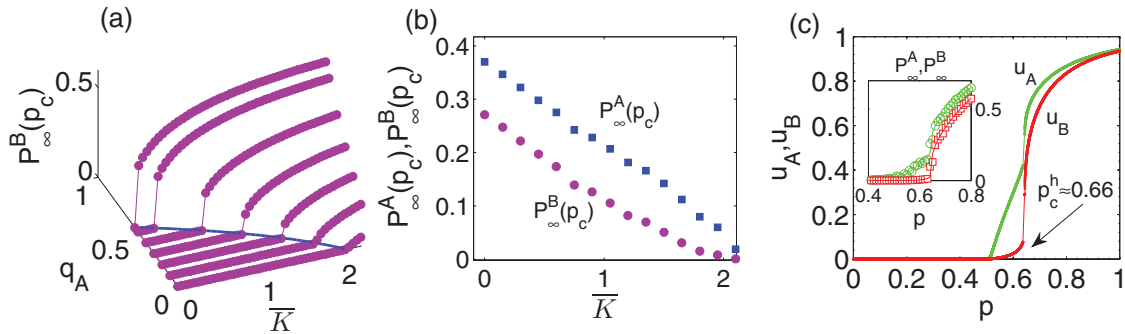


FIG. 3. (Color online) (a) Size of giant components vs dependency and connectivity links strength, for $q_B = 1$ and $\bar{k} = 3$. The giant components size at p_c changes from zero to a finite value while changing q_A and \bar{K} . When q_A and \bar{K} are at the boundary of different phase transitions, the jump occurs [see Fig. 2(b)]. (b) The values of $P_\infty^A(p_c)$ (\circ) and $P_\infty^B(p_c)$ (\square) along the boundary for $q_B = 1$ and $\bar{k} = 3$. (c) A hybrid phase transition, for $q_B = 1$, $q_A = 0.35$, $\bar{k} = 3$, and $\bar{K} = 0.1$. According to Eqs. (5), P_∞^A and P_∞^B have the same properties as u_A and u_B , respectively. At $p = p_c^h \approx 0.66$ the values of u_A and u_B jump, and then for lower p values they continuously approach zero. In the inset, simulation and theoretical results are shown as symbols and lines, respectively.

For a second-order phase transition, the giant component decreases continuously to zero at the percolation threshold p_c . Thus, by taking the limit of system (6) at $u_A = u_B = 0$ we obtain the second-order threshold:

$$p_c^{\text{II}} = \frac{1 - \bar{k}_B(1 - q_B)}{[\bar{k}_A + (\bar{k}_{BA}\bar{k}_{AB} - k_A k_B)(1 - q_B)](1 - q_A)}. \quad (8)$$

In particular for $q_A = 1$ and $0 < q_B < 1$ this threshold becomes

$$p_c^{\text{II}} = \frac{1}{\bar{k}_B(1 - q_B)},$$

which together with Eq. (7) implies that $p_c^{\text{II}} > 1$, and therefore the phase transition must be of first order at $p_c^{\text{I}} < 1$ (that will be determined later).

When extracting u_B from the first equation of system (6), it can be rewritten as

$$u_B = -\frac{\log(1 - u_A) + k_A p(1 - q_A)u_A}{k_A p q_A u_A + k_{AB}[1 - q_B(1 - p u_A)]} \equiv H_1(u_A), \quad (9)$$

$$u_B = 1 - e^{-\bar{k}_{BA} u_A p [1 - q_A(1 - u_B)] - \bar{k}_B u_B [1 - q_B(1 - u_A p)]} \equiv H_2(u_A).$$

The intersection of the two curves (the maximum solution of u_A, u_B) is the solution of the system. When the phase transition is first order and $p = p_c^{\text{I}}$, the curves of Eqs. (9) are tangentially touching at the solution point, where

$$\left. \left(\frac{dH_1}{du_A} = \frac{dH_2}{du_A} \right) \right|_{p=p_c^{\text{I}}}. \quad (10)$$

Obviously, u_A, u_B , and p can be treated as variables of Eqs. (9) and (10). Solving these equations, the minimal solution of p and the corresponding maximal u_A and u_B is the solution of the system at criticality.

B. Full dependence

When networks A and B are fully dependent, i.e., $q_A = q_B = 1$, both networks must be the same size and therefore $\bar{k}_{AB} = \bar{k}_{BA} \equiv \bar{K}$, and system (6) yields a simple

form:

$$\begin{aligned} u_A &= 1 - \exp[-pu_A u_B(\bar{k}_A + \bar{K})], \\ u_B &= 1 - \exp[-pu_A u_B(\bar{k}_B + \bar{K})]. \end{aligned}$$

The size of the mutual giant component P_∞ is thus given by

$$P_\infty = P_\infty^A = P_\infty^B = p[1 - e^{-P_\infty(\bar{k}_A + \bar{K})}][1 - e^{-P_\infty(\bar{k}_B + \bar{K})}], \quad (11)$$

which is similar to the solution of the fully interdependent system [31,34], where the only difference is that the degrees of networks A and B are now replaced by $\bar{k}_A + \bar{k}_{AB}$ and $\bar{k}_B + \bar{k}_{BA}$, respectively. Thus, interestingly, in a fully interdependent coupled networks system, adding connectivity interlinks has the same effect as increasing the intradegree of the corresponding networks and, therefore, in this case, the phase transition must be of first order. From Eqs. (9) and (10), one can get the threshold:

$$p_c^I = \frac{1}{k_A(1-u_A)[-1 + (1-u_A)^\alpha - u_A\alpha(1-u_A)^{\alpha-1}]}, \quad (12)$$

where $\alpha \equiv (\bar{k}_B + \bar{k}_{BA})/(\bar{k}_A + \bar{k}_{AB})$, and u_A satisfies the equation

$$u_A = 1 - \exp\left\{\frac{u_A[1 - (1-u_A)^\alpha]}{(1-u_A)[-1 + (1-u_A)^\alpha - u_A\alpha(1-u_A)^{\alpha-1}]}\right\}. \quad (13)$$

By substituting p_c^I from Eq. (8) into Eqs. (9) and (10) and evaluating both u_A and u_B , we can derive in the phase diagram the boundary between the first- and second-order transitions [see dashed line in Fig. 2(b)]. An interesting phenomenon, which to the best of our knowledge has not been observed before, is that when the phase transition changes from first to second order, there are discontinuities (abrupt jumps) of $P_\infty^A(p_c)$, $P_\infty^B(p_c)$ in the phase-transition boundary [see Figs. 3(a) and 3(b)]. The boundary between the first- and second-order phase transition satisfies $p_c^I = p_c^{II}$. Therefore, by replacing p_c^I by p_c^{II} in Eq. (9) and evaluating both u_A and u_B we obtain the boundary, seen in Fig. 3(a), between the first- and second-order transitions. When we reduce the three equations to a single equation, u_A, u_B should always be the maximal non-negative solution in $[0, 1]$. When Eqs. (9) and (10) have more than one solution, we always choose the minimal non-negative value p_c^{\min} and the corresponding maximal values u_A^{\max}, u_B^{\max} as the physical solution at the threshold. In part of the boundary, $u_A^{\max} > 0$ and $u_B^{\max} > 0$, and of course $p_c^{\min}, u_A = 0$, and $u_B = 0$ are also the solution of the system. This means that there exist two intersections that both satisfy the tangential condition on the boundary [as shown in Fig. 4(a)]. This implies that when the order of the phase transition changes from first to second, $P_\infty^A(p_c), P_\infty^B(p_c)$ are discontinuous [see Figs. 3(a) and 3(b)]. This phenomenon contrasts most known systems possessing both first- and second-order transitions. Usually, in physical systems, the first-order jump in the order parameter and other related properties, such as the specific heat, present a continuous change along the transition line when the system changes from first to second order [35].

In addition to the existence of jumps in $P_\infty^A(p_c), P_\infty^B(p_c)$ at the boundary between the first- and second-order phase

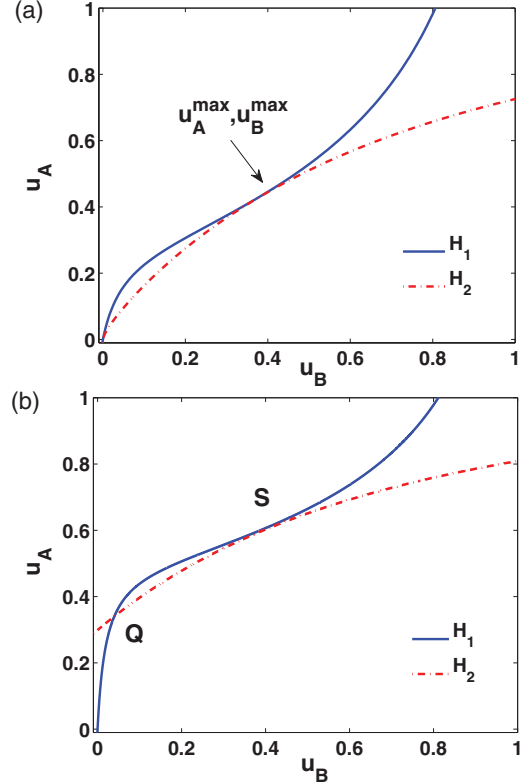


FIG. 4. (Color online) Tangential conditions. (a) An abrupt jump on the boundary for $q_A = 0.394, q_B = 0.8$ and $\bar{k} = 3, \bar{K} = 0.2$. Here $p_c^I = p_c^{II} = 0.5464$, which is the threshold of the system. Although both intersections (one of which is at the origin) satisfy the tangential condition, the u_A^{\max}, u_B^{\max} values are the physical solution and the transition is of the first order. (b) Hybrid transition analysis, for $q_B = 1, q_A = 0.35, \bar{k} = 3$, and $\bar{K} = 0.1$. Here $p_c \approx 0.556$ and $p_c^h \approx 0.66$. The maximal intersection S satisfies the tangential condition. When continuously decreasing p , the solution of the system jumps from the maximal intersection S to the minimal intersection Q and then continuously decreases to zero.

transitions, we find also another unusual phenomenon. When one network strongly depends on the other, there exist *hybrid* phase transitions. A hybrid phase transition means that, when the attack strength, $1 - p$, increases, the size of the giant component jumps at p_c^h from a large value to a small value and then continuously decreases to zero. A similar behavior has been found in bootstrap percolation [36]. Since the second-order transition is characterized by a giant component which is continuous in the neighborhood of p_c , we regard the hybrid phase-transition regime as a second-order phase-transition regime [see Fig. 2(b)]. For the hybrid phase transition, there exists a threshold p_c^h at which the jump occurs. For p just below p_c^h , the solution of Eqs. (9) for u_A, u_B will jump to lower values. After the jump, when p further decreases, u_A and u_B approach zero continuously, which implies that the giant components' sizes change to zero continuously [see Fig. 3(c)].

For the three-equation system Eqs. (9) and (10), the minimal solution of p^{\min} in $[0, [1]$ is p_c (the physical solution). Besides p^{\min} , if Eqs. (9) have another solution $p_c^h \in (0, 1)$ and corresponding solution u_A^h, u_B^h , we can find a hybrid phase

transition. The set (p^h, u_A^h, u_B^h) means that when p is just below p_c^h the solutions u_A, u_B of the first two equations of Eqs. (9) will jump to small values. After the jump, when we continue to decrease p toward $p_c = p^{\min}$, both u_A and u_B will continuously decrease to zero. For example, for the parameters $q_A = 0.35, q_B = 1, \bar{k} = 3$, and $\bar{K} = 0.1$, we obtain $p_c \approx 0.556$ and $p_c^h \approx 0.66$. When p is just below 0.66, the giant components drop to smaller positive values like in a first-order phase transition. After this discontinuous drop, the giant components' sizes continuously decrease to zero while decreasing p from 0.66 to 0.556, like a second-order phase transition [see Fig. 4(b)].

IV. SUMMARY AND CONCLUSION

In summary, we studied the dynamics of the cascading failures process and the state solutions of the giant components in coupled networks, when both interdependent and interconnected links exist, using a percolation approach. Although our detailed analysis is for ER networks, the theory can be applied to any network systems topology. We find that the existence of interconnectivity links between interdependent networks introduces rich and intriguing phenomena through the process of cascading failures. Increasing the strength of interconnecting links can significantly change the transition behavior and often brings up some counterintuitive phenomena, such as changing of the transition from second order to first order [as seen in Fig. 2(b)]. We also find an unusual abrupt jump in the boundary between first- and second-order phase transitions at the criticality. Moreover, when one of the networks strongly depends on the other network, unusual hybrid phase transitions are observed represented by continuous and discontinuous changes in the giant component.

ACKNOWLEDGMENTS

We thank Amir Bashan for helpful discussions. This work is partially supported by the Office of Naval Research, Deutsche Forschungsgemeinschaft, Defense Threat Reduction Agency, European Union project Epiwork, and the Israel Science Foundation. Y. Hu is supported by the National Science Foundation under Grants No. 60974084 and No. 60534080. R. Cohen thanks BSF for partial support.

APPENDIX: HOW TO GET $g_A(\varphi, \phi)$ AND $g_B(\varphi, \phi)$

We model the percolation process using the branching process approach. Let $\mathcal{G}_0^A(x_A, x_B) = \sum_{k_A, k_{AB}} \rho_{k_A, k_{AB}}^A x_A^{k_A} x_B^{k_{AB}}$ and $\mathcal{G}_0^B(x_A, x_B) = \sum_{k_B, k_{BA}} \rho_{k_B, k_{BA}}^B x_A^{k_{BA}} x_B^{k_B}$ be the degree distributions' generating functions. The probability of following

a randomly chosen AB link connecting an A node of degree k_A to a B node with excess k_{AB} degree (i.e., having a total A -to- B degree of $k_{AB} + 1$) is proportional to $(k_{AB} + 1) \rho_{k_A, k_{AB}}^A$, and the generating function for this distribution is [33],

$$\mathcal{G}_1^{AB}(x_A, x_B) = \sum_{k_A, k_{AB}} \frac{(k_{AB} + 1) \rho_{k_A, k_{AB} + 1}^A}{\sum_{k'_A, k'_{AB}} k'_{AB} \rho_{k'_A, k'_{AB}}^A} x_A^{k_A} x_B^{k_{AB}}. \quad (\text{A1})$$

Analogously, we construct the other three excess generating functions: $\mathcal{G}_1^{AA}(x_A, x_B)$, $\mathcal{G}_1^{BA}(x_A, x_B)$, and $\mathcal{G}_1^{BB}(x_A, x_B)$.

After removing a fraction $1 - \varphi$ of nodes in network A and a fraction $1 - \phi$ of nodes in network B , we can set new arguments to the generating functions, so that x_A and x_B will be replaced by $1 - \varphi(1 - x_A)$ and $1 - \phi(1 - x_B)$, respectively [37–39]. Suppose $g_A(\varphi, \phi), g_B(\varphi, \phi)$ are the fractions of A nodes and B nodes in the giant components after removal of $1 - \varphi$ and $1 - \phi$ fractions of networks A and B , respectively. Then we have

$$\begin{aligned} g_A(\varphi, \phi) &= 1 - \mathcal{G}_0^A[1 - \varphi(1 - f_A), 1 - \phi(1 - f_{BA})], \\ g_B(\varphi, \phi) &= 1 - \mathcal{G}_0^B[1 - \varphi(1 - f_{AB}), 1 - \phi(1 - f_B)], \end{aligned} \quad (\text{A2})$$

where

$$\begin{aligned} f_A &= \mathcal{G}_1^{AA}[1 - \varphi(1 - f_A), 1 - \phi(1 - f_{BA})], \\ f_{AB} &= \mathcal{G}_1^{AB}[1 - \varphi(1 - f_A), 1 - \phi(1 - f_{BA})], \\ f_{BA} &= \mathcal{G}_1^{BA}[1 - \varphi(1 - f_{BA}), 1 - \phi(1 - f_B)], \\ f_B &= \mathcal{G}_1^{BB}[1 - \varphi(1 - f_{BA}), 1 - \phi(1 - f_B)]. \end{aligned} \quad (\text{A3})$$

When all degree distributions of inter- and intranetworks A and B are Poissonian distributed, all the functions can be more simple. Assume \bar{k}_A and \bar{k}_B are the average intralinks degrees in networks A and B and $\bar{k}_{AB}, \bar{k}_{BA}$ are the average interlinks degrees between A and B (allowing the case $\bar{k}_{AB} \neq \bar{k}_{BA}$, since the network sizes of A and B can be different), then we have $\mathcal{G}_0^{AA}(x_A) = e^{\bar{k}_A(x_A - 1)}$, $\mathcal{G}_0^{AB}(x_B) = e^{\bar{k}_B(x_B - 1)}$, $\mathcal{G}_0^{BA}(x_A) = e^{\bar{k}_{BA}(x_A - 1)}$, $\mathcal{G}_0^{BB}(x_B) = e^{\bar{k}_B(x_B - 1)}$, and

$$\begin{aligned} \mathcal{G}_1^{AA}(x_A, x_B) &= \mathcal{G}_1^{AB}(x_A, x_B) = \mathcal{G}_0^A(x_A, x_B) \\ &= \mathcal{G}_0^{AA}(x_A) \mathcal{G}_0^{AB}(x_B), \\ \mathcal{G}_1^{BB}(x_A, x_B) &= \mathcal{G}_1^{BA}(x_A, x_B) = \mathcal{G}_0^B(x_A, x_B) \\ &= \mathcal{G}_0^{BA}(x_A) \mathcal{G}_0^{BB}(x_B). \end{aligned} \quad (\text{A4})$$

Submitting the above equations into systems (A2) and (A3), we get

$$\begin{aligned} g_A(\varphi, \phi) &= 1 - \exp[-\bar{k}_A x g_A(\varphi, \phi) - \bar{k}_{AB} y g_B(\varphi, \phi)], \\ g_B(\varphi, \phi) &= 1 - \exp[-\bar{k}_{BA} x g_A(\varphi, \phi) - \bar{k}_B y g_B(\varphi, \phi)]. \end{aligned} \quad (\text{A5})$$

- [1] A.-L. Barabási and R. Albert, *Science* **286**, 509 (1999).
 [2] D. J. Watts and S. H. Strogatz, *Nature (London)* **393**, 440 (1998).
 [3] R. Albert and A.-L. Barabási, *Rev. Mod. Phys.* **74**, 47 (2002).
 [4] Y. Hu, Y. Wang, D. Li, S. Havlin, and Z. Di, *Phys. Rev. Lett.* **106**, 108701 (2011).

- [5] C. Song, S. Havlin, and H. A. Makse, *Nature (London)* **433**, 392 (2005).
 [6] R. Pastor-Satorras and A. Vespignani, *Evolution and Structure of the Internet: A Statistical Physics Approach* (Cambridge University Press, Cambridge, 2006).

- [7] S. N. Dorogovtsev and J. F. F. Mendes, *Evolution of Networks: From Biological Nets to the Internet and WWW* (Oxford University Press, New York, 2003).
- [8] A. Barrat, M. Barthélemy, and A. Vespignani, *Dynamical Processes on Complex Networks* (Cambridge University Press, Cambridge, 2008).
- [9] D. S. Callaway, M. E. J. Newman, S. H. Strogatz, and D. J. Watts, *Phys. Rev. Lett.* **85**, 5468 (2000).
- [10] R. Cohen, K. Erez, D. ben-Avraham, and S. Havlin, *Phys. Rev. Lett.* **85**, 4626 (2000); **86**, 3682 (2001).
- [11] M. E. J. Newman, *Networks: An Introduction* (Oxford University Press, Oxford, 2010).
- [12] S. H. Strogatz, *Nature (London)* **410**, 268 (2001).
- [13] D. J. Watts, *Proc. Natl. Acad. Sci. USA* **99**, 5766 (2002).
- [14] M. E. J. Newman and M. Girvan, *Phys. Rev. E* **69**, 026113 (2004).
- [15] C. Song, S. Havlin, and H. A. Makse, *Nature Physics* **2**, 275 (2006).
- [16] M. Tumminello, F. Lillo, and R. N. Mantegna, *Europhys. Lett.* **78**, 30006 (2007).
- [17] G. Caldarelli and A. Vespignani, *Large Scale Structure and Dynamics of Complex Webs* (World Scientific, New York, 2007).
- [18] A. Barrat, M. Barthélemy, and A. Vespignani, *Dynamical Processes on Complex Networks* (Cambridge University Press, Cambridge, 2008).
- [19] M. Barthélemy, *Physics Reports* **499**, 1 (2010).
- [20] D. Li, K. Kosmidis, A. Bunde, and S. Havlin, *Nature Physics* **7**, 481 (2011).
- [21] R. Albert, H. Jeong, and A. L. Barabási, *Nature (London)* **406**, 378 (2000).
- [22] R. Milo, S. Shen-Orr, S. Itzkovitz, N. Kashtan, D. Chklovskii, and U. Alon, *Science* **298**, 824 (2002).
- [23] L. K. Gallos, R. Cohen, P. Argyrakis, A. Bunde, and S. Havlin, *Phys. Rev. Lett.* **94**, 188701 (2005).
- [24] S. Boccaletti, V. Latora, Y. Moreno, M. Chavez, and D. U. Hwang, *Phys. Rep.* **424**, 175 (2006).
- [25] R. Cohen and S. Havlin, *Complex Networks: Structure, Robustness and Function* (Cambridge University Press, England, 2010).
- [26] V. Rosato *et al.*, *Int. J. Crit. Infrastruct.* **4**, 63 (2008).
- [27] N. K. Svendsen and S. D. Wolthusen, *Information Security Technical Report* **21**, 44 (2007).
- [28] S. M. Rinaldi, J. P. Peerenboom, and T. K. Kelly, *IEEE Control Syst. Mag.* **21**, 11 (2001).
- [29] J. Peerenboom *et al.*, in Proc. CRIS/DRM/IIIT/NSF Workshop Mitigat. Vulnerab. Crit. Infrastruct. Catastr. Failures (2001).
- [30] J.-C. Laprie, K. Kanoun, and M. Kaâniche, *Computer Safety, Reliability, and Security* **4680**, 54 (2007).
- [31] S. V. Buldyrev, R. Parshani, G. Paul, H. E. Stanley, and S. Havlin, *Nature (London)* **464**, 1025 (2010).
- [32] R. Parshani, S. V. Buldyrev, and S. Havlin, *Phys. Rev. Lett.* **105**, 048701 (2010).
- [33] E. A. Leicht and R. M. D'Souza, e-print [arXiv:0907.0894](https://arxiv.org/abs/0907.0894).
- [34] J. Gao, S. V. Buldyrev, S. Havlin, and H. Eugene Stanley, *Phys. Rev. Lett.* **107**, 195701 (2011).
- [35] R. K. Pathria, *Statistical Mechanics* (Elsevier, Singapore, 2003).
- [36] G. J. Baxter, S. N. Dorogovtsev, A. V. Goltsev, and J. F. F. Mendes, *Phys. Rev. E* **82**, 011103 (2010).
- [37] M. E. J. Newman, *Phys. Rev. E* **66**, 016128 (2002).
- [38] J. Shao, S. V. Buldyrev, R. Cohen, M. Kitsak, S. Havlin, and H. E. Stanley, *Europhys. Lett.* **84**, 48004 (2008).
- [39] J. Shao, S. V. Buldyrev, L. A. Braunstein, S. Havlin, and H. E. Stanley, *Phys. Rev. E* **80**, 036105 (2009).